

Gene-Induced Drug Repurposing for Gastric Adenocarcinoma by Machine Learning

Zhijian Mao

Rutgers Preparatory School, Somerset, NJ, USA
Email: williammao001@gmail.com

Abstract—Gastric Cancer (GC) is one of the leading causes of cancer death worldwide. Drug repurposing plays a critical role in rapid drug discovery to resist the growth of tumor cells. In this project, we developed a computational drug repurposing pipeline (RepoGC) for gastric adenocarcinoma based on bulk-RNA transcriptomics profiles. With the gene expression profile of gastric cancer from the Gene Expression Omnibus (GEO), a total of 1004 differentially expressed genes were identified and used for the generation of potential drug targets. Over 10,000 drugs from DrugBank were used as drug candidates. The multi-omics networks, such as gene-gene interaction and gene-target interaction network, were constructed to discover the core genes and targets for repurposed drugs and assist drug ranking. We performed the drug-target interaction prediction by deep neural network to prioritize the repurposed drugs. Finally, a combined drug-target interaction score was generated to rank drug candidates. Among the top-ranked drugs, such as Ursolic acid, Geldanamycin, and Parthenolide, we explored their completed clinical trial evidence and studies in the field of gastric cancer to cross validate the drugs. The study presents an efficient computational method to integrate transcriptomics data for rapid drug repurposing. The project highlights the potential of RepoGC to identify new drugs for gastric adenocarcinoma.

Keywords—drug repurposing, machine learning, transcriptomics, gastric cancer

I. INTRODUCTION

Gastric Cancer (GC) is the fifth common cancer and one of the major causes of cancer death globally, in which cells in the stomach grow uncontrollably and spread to other parts of the body [1]. More than one million people worldwide were diagnosed with gastric cancer every year (Fig. 1) [2].

Many therapeutic strategies are available to alleviate the progression of gastric cancer, including chemotherapy, surgery, radiation therapy, and hormone therapy. The development of drugs is often accompanied with these therapies to combat cancer cells. Drug repurposing strategy is an effective approach to propose existing drugs to resist the growth of cancer cells. Drug repurposing offers significant advantages, including

reducing costs and saving time for drug development [3], [4], increasing success rates for bringing new treatments to diseases [4, 5], and the ability to target previously untreatable diseases (Fig. 2) [6]. Additionally, repurposing drugs that have already undergone extensive safety testing can reduce the risk of unexpected side effects and increase the speed of getting treatments to patients in need [7–10].

Gene expression induced drug repurposing is an effective method for drug discovery [1, 11]. It refers to the process of finding new therapeutic uses for existing drugs by analyzing changes in gene expression patterns caused by the drug in disease tissue [12]. Transcriptome data can help identify new therapeutic targets that have beneficial effects on targeted therapy. In addition, genome data and drugs can help researchers in reposition the use of studied drugs and study their molecular mechanisms by building a drug disease interaction network [13, 14]. The characteristics of a drug can be derived from three general types of data: transcriptome (RNA) proteome or metabolome data, chemical structure, and adverse event profiles [15]. Matching transcriptome signatures can be used for drug-disease comparison (estimating drug-disease similarity) [16] and drug-drug comparison [17]. In the comparison of drugs and diseases, the transcriptome characteristics of specific drugs are obtained by comparing the gene expression profiles of biomaterials before and after drug treatment, and then comparing the differential gene expression characteristics with the disease related expression profiles obtained through differential expression analysis of target diseases and health conditions. The differentially expressed genes provide candidates for drug targets. The interaction between drugs and their respective targets is the reason for therapeutic effects, which helps to overcome the diseases targeted by drug development. The target may be a protein (or gene) directly related to the disease, or a protein whose disturbance indirectly helps to offset the protein causing the disease [2]. In any case, the interaction is worth studying because the therapeutic effect of drugs is achieved through it. Due to the large number of drug targets, effective screening of drug target pairs is critical for ranking the repurposed drugs. Drug-target interaction prediction is an efficient approach to rank the drug-target pairs by predicting the binding affinity.

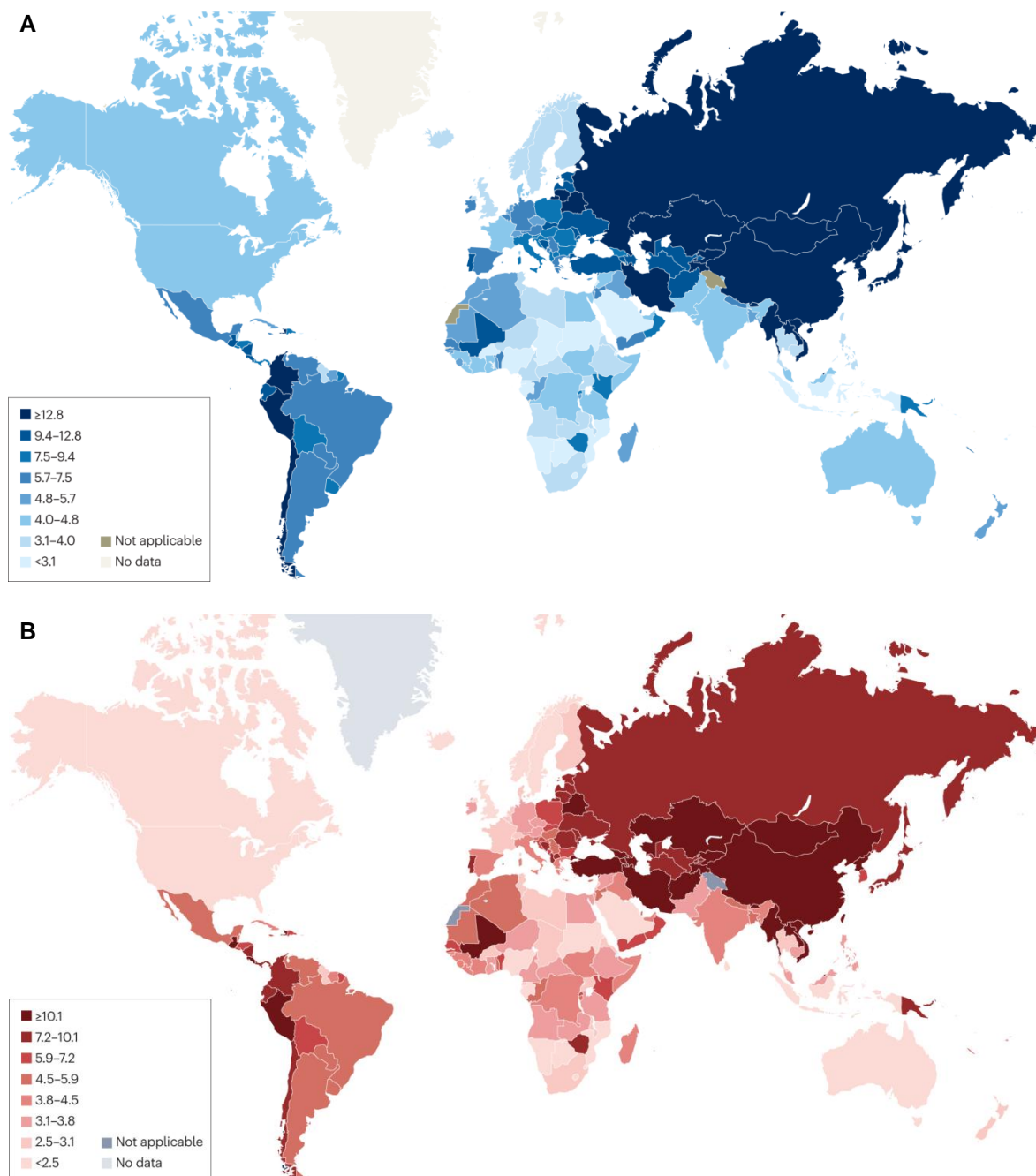


Fig. 1. Worldwide gastric cancer incidence and mortality in 2020. Panel A shows the estimated number of age-standardized incidence rates per 100,000 persons based on data from GLOBOCAN 2020. Panel B shows the estimated age-standardized death rates per 100,000 population based on GLOBOCAN 2020 data.

In this project, we developed a computational drug repurposing method for gastric adenocarcinoma based on transcriptome characteristics by designing an end-to-end computing pipeline (RepoGC). We used transcriptome data from the Gene Expression Omnibus (GEO) to obtain a total of 1004 differential genes in 389 GC samples for gastric adenocarcinoma. We identified core correlation

and functional genes as potential drug targets through gene enrichment analysis by ShinyGO. We also inferred the maximum target of interaction through the Protein-Protein Interaction (PPI) network. Finally, we selected the top candidate drugs with goals for further evaluation, explored and verified the feasibility of them through the iLINC database.

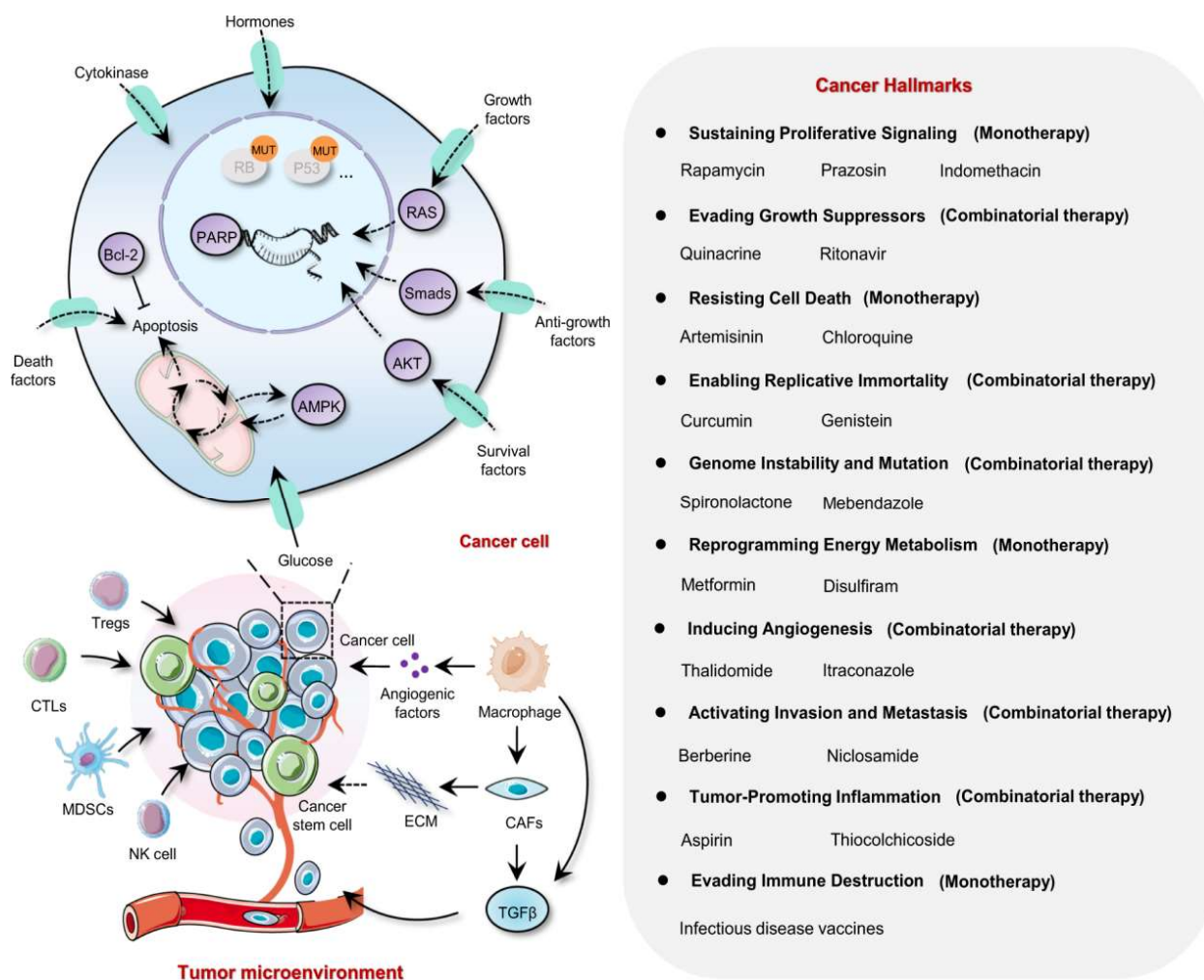


Fig. 2. The drug development for cancer by drug repurposing approach. The identification of drug candidates targeting the hallmarks of the cancer cell using drug repurposing enabled by recapitulative signaling networks.

II. METHODS

A. Dataset

We selected four transcriptomics profiles related to gastric cancer from the GEO database, namely: GSE13911 and GSE54129. GSE13911 dataset contains 69 RNA-seq data with gene expression data from 38 primary gastric cancer samples and 31 adjacent normal samples. GSE19826 dataset contains 27 RNA-seq data with gene expression data from 12 adjacent normal or tumor-matched gastric tissues and 3 normal tissue samples. GSE54129 dataset contains 132 RNA-seq data with gene expression data from 111 primary gastric cancer samples and 21 adjacent normal samples. GSE118916 dataset contains 30 RNA-seq data with gene expression data from 15 pairs of GAC tumor and adjacent normal tissues. We performed exploration, secondary sampling, and integration of the four microarray GEO datasets, all of which utilized the same platform GPL570. During the differential gene expression analysis of GSE13911, GSE19826, GSE54129, and GSE118916, we designated gastric tumor tissue as case group and compared it to noncancer tissue, which served as normal group. We obtained the genes with the most differentially

expressed profiles between the selected groups and generated the corresponding volcano plots to visualize the results. Subsequently, by searching for corresponding DEG IDs on GEOexplorer, we obtained information on 1004 Differentially Expressed Genes (DEGs) associated with these four gene expression profiles. The corresponding drug targets were mapped by using the genes on the Uniprot database. Over 10,000 drugs with structures were downloaded from DrugBank, which were used for virtual screening.

B. Gene Enrichment Analysis

Gene enrichment analysis was used to map a set of genes on a number of functional pathways, which aimed to identify biological functions and pathways associated with differentially expressed genes. It involves comparing the input gene list to curated gene sets from databases like GO or KEGG using statistical tests. Significant enrichment indicates potential biological relevance and provides insights into underlying molecular mechanisms. In the study, graphical gene set enrichment analysis was obtained by ShinyGO online [18]. For human genes, the program obtained pathway data from MSigDB [19], GeneSetDB [20], Reactome [21] and many verified or

predicted miRNA and TF target gene sources. ShinyGO used the pathview Bioconductor package to retrieve the path map from the KEGG web server [22] through API access to build a network view and hierarchical clustering tree with rich gene sets. ShinyGO plotted the chromosome positions of all genes in the user list, and performed statistical analysis on genome characteristics. Finally, the program plotted the distribution of GC content, as well as the length of coding sequence, transcript, and UTRs. A t-test was performed to determine any significant differences between the queried gene and all other background genes in the genome. After inputting the obtained protein information, the Pathway database was set to GO Biological Process, where the FDR cutoff was 0.05 and the Pathway size was 20 to 2000.

C. Generation of Drug Candidates from DrugBank

DrugBank (www.drugbank.ca) is an online database containing molecular information about drugs, their mechanisms, interactions, and targets. It is a fully searchable web resource with numerous built-in tools and functionalities for viewing, sorting, and extracting drug or drug-target data, facilitating in-depth analysis of drug actions and mechanisms. DrugBank's user-friendly interface and regular updates ensure access to the latest reliable information, making it an indispensable tool for researchers, clinicians, and the pharmaceutical industry in drug discovery, development, and therapeutic applications. In this study, all drugs with molecular information such as structure, clinical evidence were extracted.

D. Featurization of Drug and Protein Targets

We convert drug structures from SMILE strings to molecular fingerprints [23]. Extended-Connectivity Fingerprints (ECFPs) are a class of featurization that combines several useful molecular features [24]. They take molecules of arbitrary size and convert them into fixed-length vectors. ECFPs take molecules of many different sizes and use them all with the same model. Each element of the fingerprint vector indicates the presence or absence of a particular molecular feature, defined by some local arrangement of atoms. Each unique combination of these properties is a feature, and the corresponding elements of the vector are set to 1 to indicate their presence. The RDKit library was used to compute ECFP fingerprints for molecules. Seq2Vec is used to represent protein sequences as continuous vector embeddings in a high-dimensional space [25]. These embeddings capture semantic information about the amino acids and their relationships based on co-occurrence patterns in a large dataset of protein sequences.

E. Drug Target Interaction Prediction by DeepPurpose

DeepPurpose takes the Simplified Molecular-Input Line-Entry System (SMILES) string and protein amino acid sequence pair of compounds as input [26]. Then, through a depth conversion function, the program maps

the compounds and proteins to vector representations as described above. Then, the program will embed the learned protein and composite into the MLP decoder to generate a prediction, and then return the prediction score, representing the probability of binding between the predicted compound and protein. DeepPurpose will train five machine learning models and generate aggregate forecast results and descriptive ranking lists [26], including Support Vector Machine (SVM), logistic regression, Stochastic Gradient Descent (SGD), random forest, and K-Nearest Neighbors (KNN).

III. RESULTS

A. Framework of Drug Repurposing for Gastric Cancer

Fig. 3 shows the Framework of drug repurposing for gastric cancer. By accessing the GEO database, we obtained the multiple transcriptomics data. We reported a total of 1004 differentially expressed genes related to gastric cancer and downloaded over 10,000 drugs with structures from DrugBank. The corresponding drug targets were mapped by using the genes on the Uniprot database. We then performed functional analysis to obtain the pathway enrichment using the differentially expressed genes. Next, we used the improved DeepPurpose algorithm to predict the interactions between drugs and binding targets. Through DeepPurpose, we obtained the binding score data of 3 million DTI, among which we selected the top 10% as representative analysis and drug pool. Firstly, through the frequency of drugs, we found the top ten drugs with the highest frequency in the pool. Secondly, by using protein-protein interaction network, we chose the targets that have the largest number of degrees since they have more interactions with proteins. Finally, we explored the clinical evidence via iLINC's signature matching for drug development of gastric cancer of those drugs and targets by literature referencing. We selected the top 10% of the drugs with the highest score and selected the most common 10 drugs by comparing their incidence.

B. Differentially Gene Expression Analysis and Functional Analysis

We identified 1004 Differentially Expressed Genes (DEGs) and enriched 989 disrupted functional pathways by ShinyGO. Fig. 4 shows the DEG analysis and volcano plot for GC patients and healthy control group using data GSE13911 and GSE54129. It is observed that significant differentially expressed genes exist between gastric cancer tissue and healthy control.

We then performed functional enrichment analysis to explore whether the identified DEGs were involved in the molecular networks related to the pathogenesis of GC. As shown in Fig. 5A and 5B, we conducted enrichment analysis using the KEGG pathway and GO molecular function for the DEGs. The bar graph displays significantly enriched functional categories sorted by p-values and enrichment score. Enrichment analysis conducted on the DEGs revealed a total of 8 and 20 significantly enriched in the KEGG and GO pathways, respectively. In the development of GC, the most

significantly altered pathways in KEGG include “Protein digestion and absorption”, “Gastric acid secretion”, and “Hippo signaling pathway”. These pathways have been convincingly established to have a correlation with cancer. In the case of Gastric acid secretion, insufficient gastric acid was implicated in carcinogenesis [27]. Regarding the Hippo signaling pathway, its dysregulation can facilitate the occurrence and progression of gastric cancer [28]. In addition, the most significantly altered pathways in GO molecule function include “Phenanthrene 9, 10-

monooxygenase activity”, “Trans-1,2-dihydrobenzene-1,2-diol dehydrogenase activity”, “Indanol dehydrogenase activity”, and “P-type potassium: proton transporter activity”. Finally, we generated a network diagram using enrichment analysis to visualize the relationships between enriched pathways for these genes. The associations between these pathways were analyzed based on the overlapping genes. If two pathways (nodes) share 20% (default) or more genes, they are considered connected.

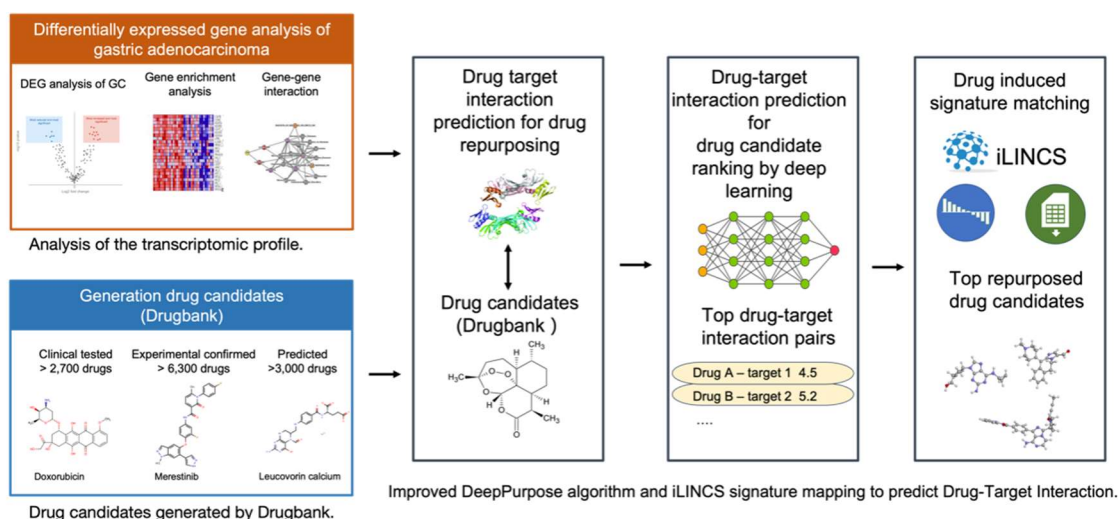


Fig. 3. Framework of gene expression-induced drug repurposing for gastric cancer.

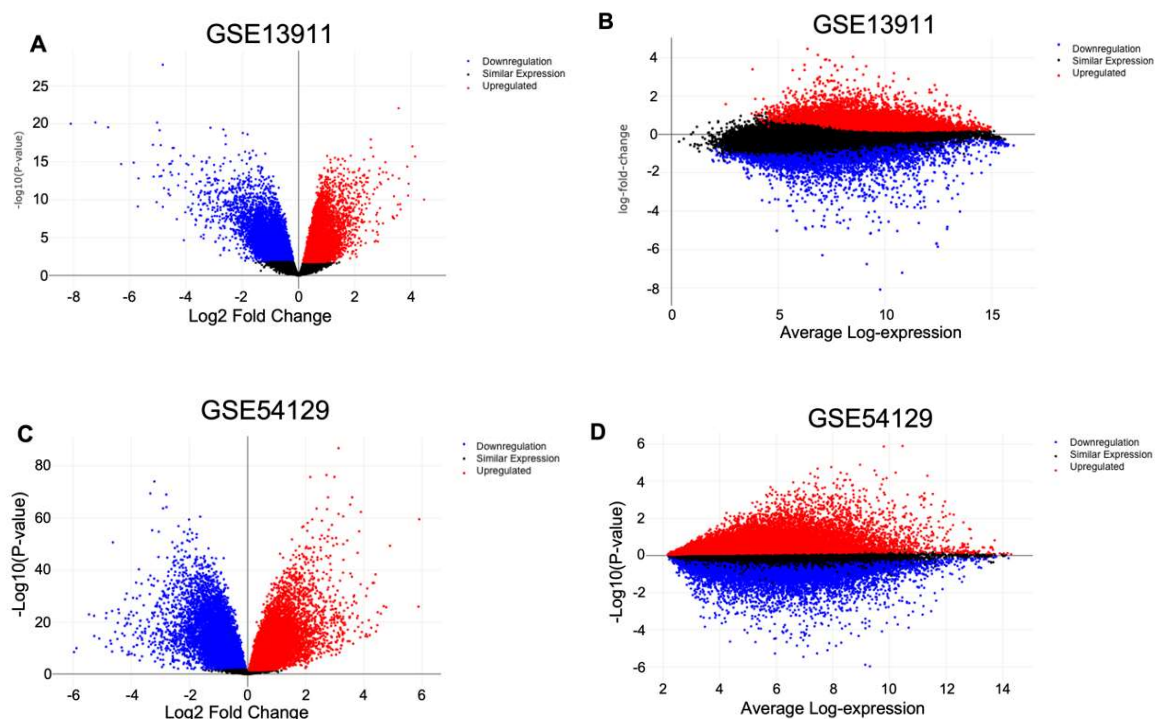
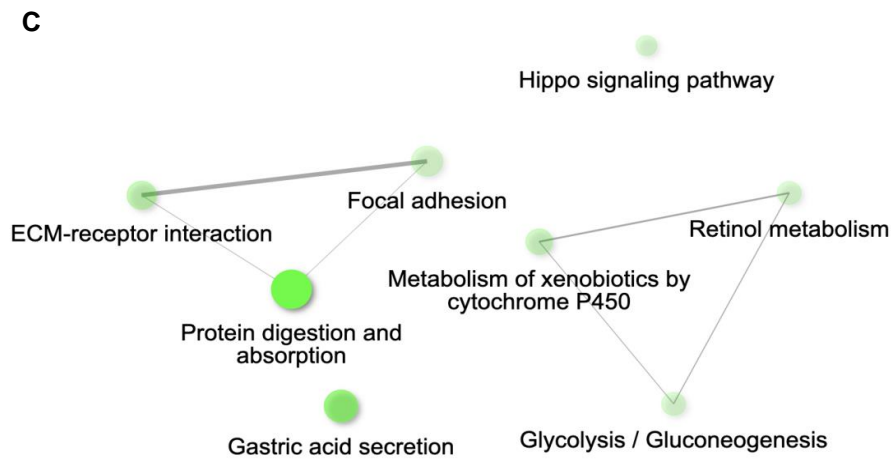
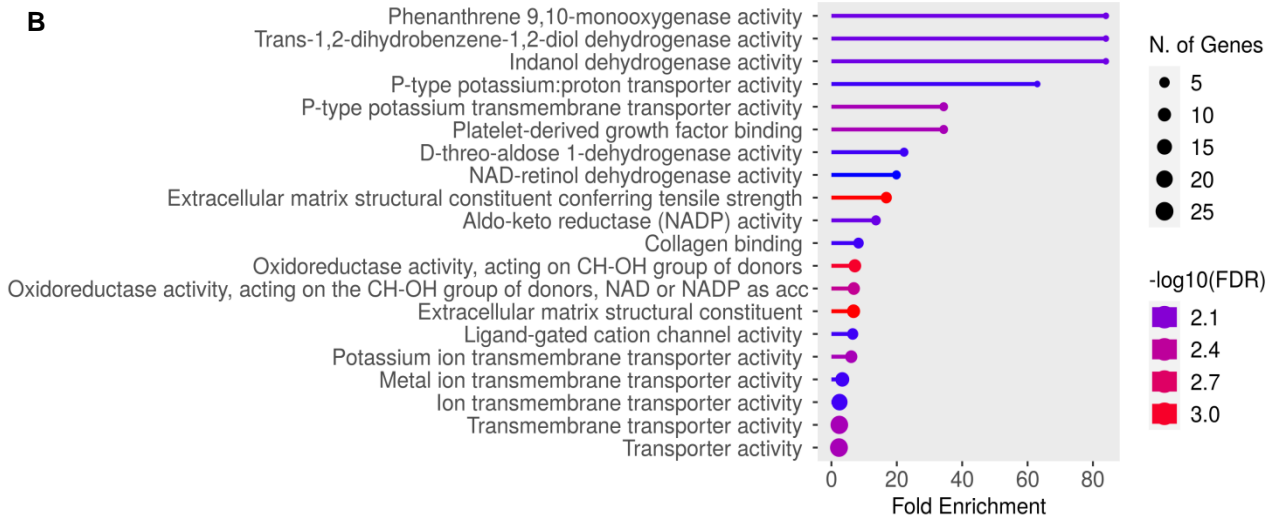
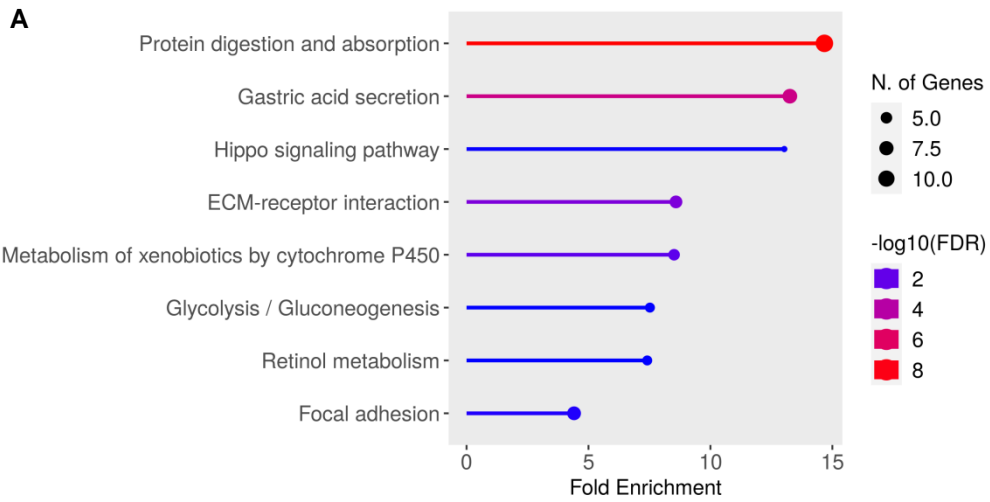


Fig. 4. Volcano plots and Mean Difference (MD) plots for GSE13911 (A, B) and GSE54129 (C, D). The volcano plot illustrates statistical significance ($-\log_{10} p$ -value) in relation to the magnitude of change (\log_2 fold change). The red and blue dots reveal the up- and down-regulated DEGs, the black dots reveal non-significant genes. On the other hand, the MD plot displays the \log_2 fold change compared to the average \log_2 expression values, providing a useful visualization for identifying differentially expressed genes.



D

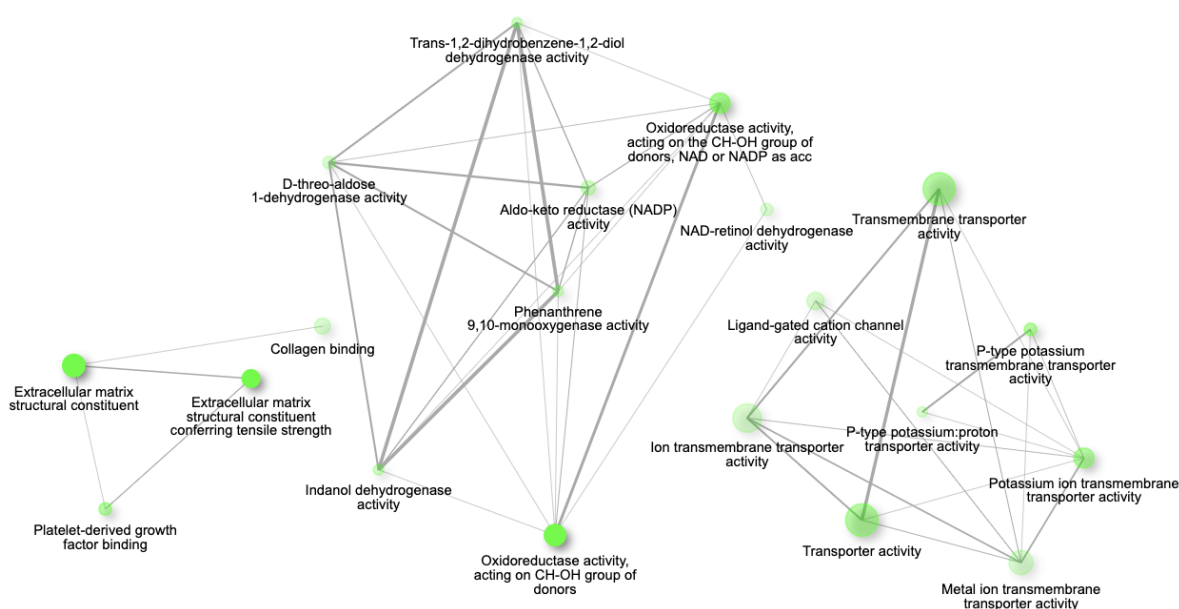


Fig. 5. Functional enrichment based on the differentially expressed genes. Panel A and B show the pathway enrichment using the KEGG (A) and GO (B) pathway database. Panel C and D show the pathway network using the KEGG (A) and GO (B) pathway database. The circumference of the nodes is proportional to the size of the gene set. The color intensity of the nodes is proportional to their enrichment significance. The thickness of the edges is proportional to the degree of overlap in gene sets.

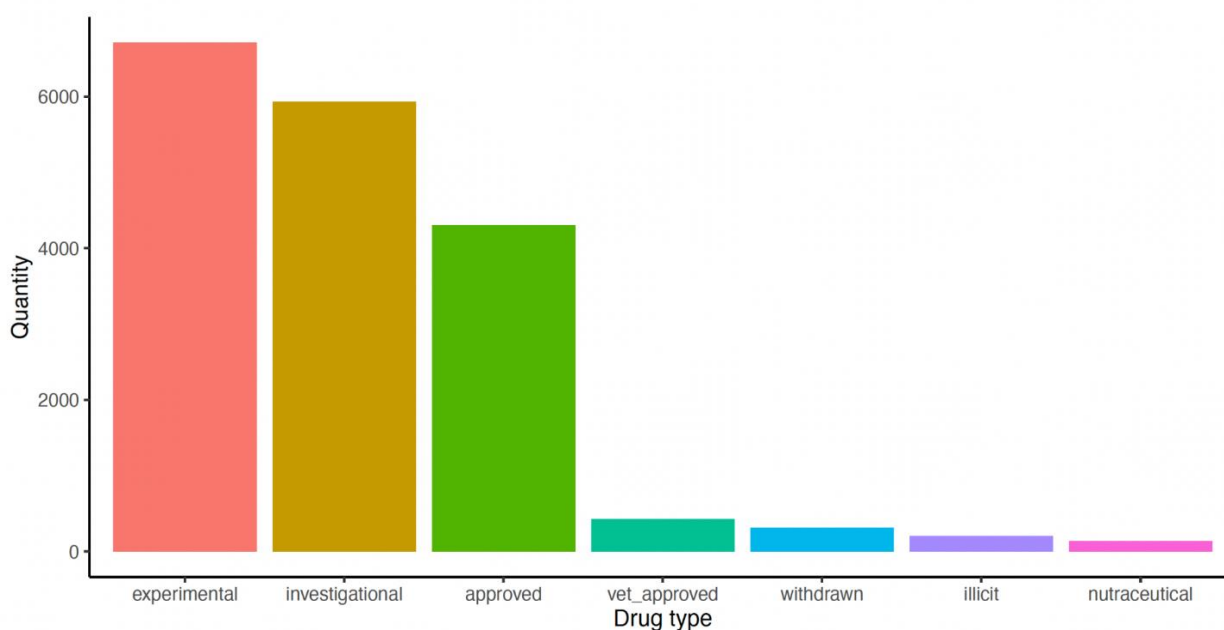
C. Exploration of Drug Candidate Patterns

Using DrugBank, we have generated the 11,912 drug candidates. Fig. 6A illustrates the distribution of drug types, where the horizontal axis represents the drug categories, and the vertical axis represents the quantity. It is evident that the majority of candidate drugs are in the experimental or research stages. Fig. 6B displays the drug

molecular categories of the candidate drugs, with the horizontal axis representing the quantity and the vertical axis representing the drug categories. It can be observed that Organoheterocyclic compounds, Benzenoids, and Organic acids and derivatives are the three most frequently occurring categories.

A

Distribution of drug types



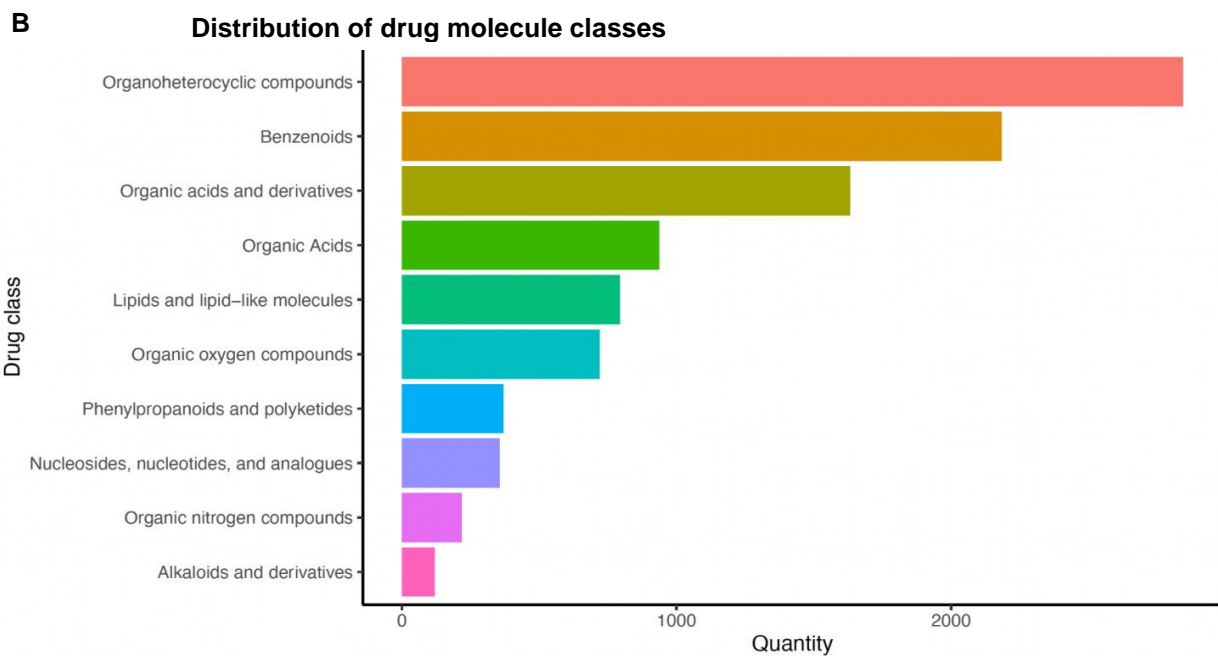


Fig. 6. The distribution of drug candidates from DrugBank. Panel A shows the distribution of drug clinical phase. Panel B shows the distribution of drug molecule classes.

D. Generation of Drug Candidates by DeepPurpose and iLINC5

We utilized DeepPurpose to measure drug-target interactions, specifically the binding of drug molecules with protein targets. By inputting Simplified Molecular-Input Line-Entry System (SMILES) strings for drugs and amino acid sequences for targets, the model generates a binding score for each drug. After selecting the top 10% of drug-target interaction structures and ranking them, we obtain the results for candidate drugs. L1000 is a dataset based on the Library of Integrated Network-based Cellular Signatures (LINCS), encompassing over one

million gene expression profiles of human cell lines subjected to chemical perturbations. L1000CDS2 serves as a web search engine based on L1000 signatures, offering prioritized pairs of small molecule features. Leveraging our previously acquired gene expression data, we input our own gene expression signature and employed L1000 to predict potential candidate drugs capable of reversing gene expression features (Fig. 7). Based on the differentially expressed gene signature mapping, 17 drugs were found to be highly correlated with the treatment of gastric cancer.

L1000CDS² An ultra-fast LINCS L1000 Characteristic Direction Signature Search Engine 860,625 searches performed

A

up genes

- SNORD110
- CTSB
- MFAP2
- FNT1
- ZNFND19
- HMGB3P1
- PGM2
- SPP1
- AGAP2-AS1
- NID2
- GRINA
- SERPINH1
- MTHFD1L
- NIHRS14

down genes

- SOSTDC1
- SCNN1B
- ACER2
- ADTRP
- TMEM116
- PPID
- PBLD
- C16orf89
- KCNE2
- PGA5
- SCARAS
- ID4
- ADH1A
- YIE1R

Search

Examples and Signatures

Select a demo example or a pre-computed signature as input:

Gene-set Example
EBOV Signatures
Disease Signatures

Signature Example
Ligand Signatures
CCLE Signatures

Configuration

reverse Search for small molecule signatures that reverse my input.

latest The database version to be used for search.

Search for small molecule combinations.

Including more small molecules in the signature search.

Yes, I agree to share my input signature and metadata for search by other investigators.

Metadata

Tag

Cell

Perturbation

Time point

+

Recent Searches

- Cancer of the stomach_gse2685 (reverse)
- Gene-set Example (reverse)
- 2313287 (reverse)
- Cancer of the stomach_gse2685 (reverse)
- Stomach cancer_gse49515 (reverse)
- [More...](#)

* Recent searches are stored in the browser's local storage. Clearing browsing data would result in a loss of these records.

L1000CDS² is being developed by the Ma'ayan Lab at the Icahn School of Medicine at Mount Sinai for the BD2K-LINCS DCIC and the KMC-IDG. The L1000CDS² tool underlying dataset is the LINCS L1000 small molecule expression profiles generated at the Broad Institute by the Connectivity Map Group. This work is supported by NIH Grants U54HL127824 and U54CA189201.

B

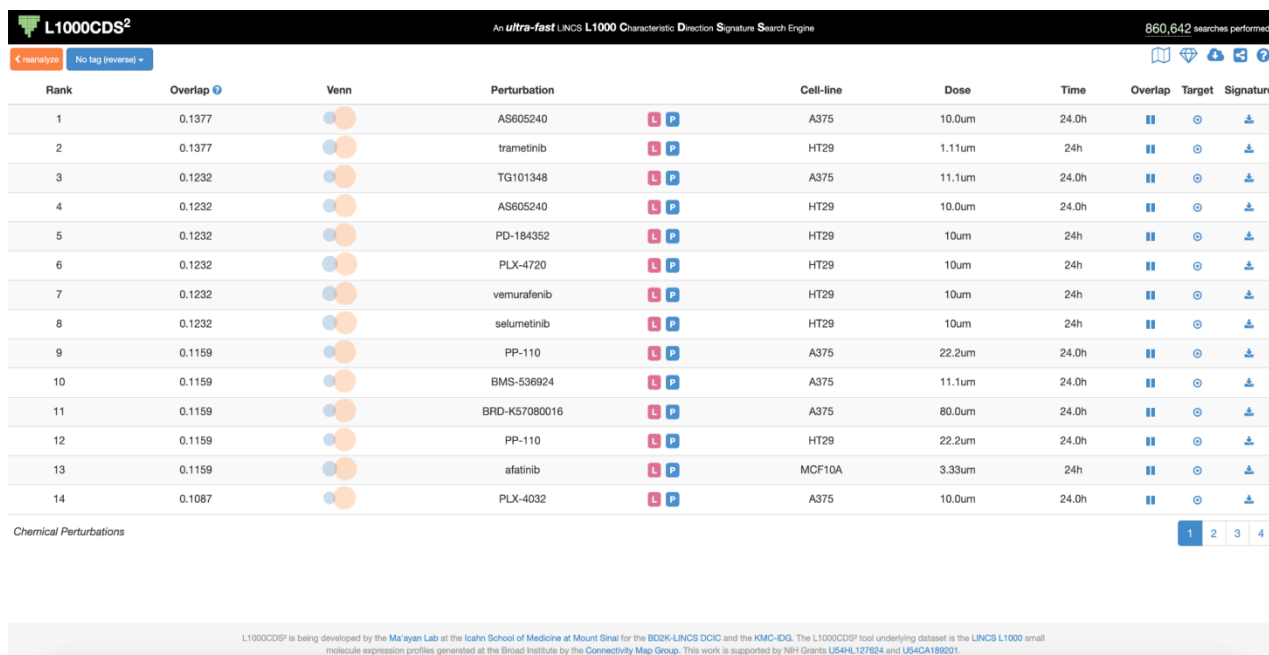


Fig. 7. The process employing the L1000 Characteristic Direction Signature Search Engine (L1000CDS2) for drug candidate prioritization. Panel A showcases the main interface post input of up-regulated genes and down-regulated genes, wherein the configuration options entail selecting small molecule signatures contrary to the input. Panel B presents the resultant data obtained post-search.

TABLE I. TOP DRUG CANDIDATES GENERATED BY DEEPPURPOSE AND ILINCS

Drug Name	Protein names	Gene Names	Target Name	Binding Score	Validation by experimental study
Ursolic acid	Monofunctional C1-tetrahydrofolate synthase, mitochondrial	MTHFD1L	Q6UB35	7.09	[29]
Testosterone propionate	Protein-tyrosine-phosphatase	PTPRS	G8JL96	6.87	N/A
Geldanamycin	Integral membrane protein GPR155	GPR155	Q7Z3F1	6.52	[30]
Levonorgestrel	Formate--tetrahydrofolate ligase	MTHFD1L	B7ZM99	6.52	N/A
Radicicol	Monofunctional C1-tetrahydrofolate synthase, mitochondrial	MTHFD1L	Q6UB35	6.31	N/A
Parthenolide	Protein-tyrosine-phosphatase	PTPRS	G8JL96	6.29	[31]
Selumetinib	Formate--tetrahydrofolate ligase	MTHFD1L	B7ZM99	6.16	[32]
Tivantinib	Kinesin family member 26B	KIF26B	B7WPD9	6.13	[33]
Trametinib	Protein-tyrosine-phosphatase	PTPRS	G8JL96	6.08	[34]
Vorinostat	Kinesin-like protein KIF26B	KIF26B	Q2KJY2	6.05	[35]
Isoliquiritigenin	Protein tyrosine phosphatase, receptor type, S, isoform CRA_a	PTPRS	D6W633	6.03	[36]
Dasatinib	Monofunctional C1-tetrahydrofolate synthase, mitochondrial	MTHFD1L	Q6UB35	5.91	[37]
Vemurafenib	Nidogen-2 (NID-2)	NID2	Q14112	5.82	[38]
Tegaserod	Serine/threonine-protein kinase 3	STK3 KRS1 MST2	Q13188	5.78	[39]
Afatinib	Nucleolar GTP-binding protein 1	GTPBP4	D2CFK9	5.77	[40]
Canertinib	Kinesin-like protein KIF26B	KIF26B	Q2KJY2	5.77	N/A
Crizotinib	Collagen, type XII, alpha 1	COL12A1	B9EJB8	5.69	[41]

Then we further pooled out the drug-target interaction scores and obtained the top ranked drug list as shown in Table I. Furthermore, we conducted a reverse search using existing candidate drugs against other gastric cancer disease signatures. By combining these datasets, we identified signature profiles that we believe could modify the gastric cancer gene expression signature.

E. Repurposed Drug of Gastric Cancer

As a result, we have identified several candidate drugs with repositioning potential, including Ursolic acid,

Testosterone propionate, Geldanamycin, Levonorgestrel, Radicicol, Parthenolide, Selumetinib, Tivantinib, Trametinib, and Vorinostat. Most of the drug candidates have prior studies to show the feasibility that they can be used for gastric cancer. Among these drugs, Ursolic acid, a pentacyclic triterpenoid, effectively inhibits the growth of gastric cancer cells *in vitro*, significantly increasing apoptosis rates in both *in vitro* and *in vivo* treated tumor cells [29]. Geldanamycin, an ansamycin antitumor antibiotic, suppresses Hsp90 function and induces apoptosis in human gastric cancer cells by affecting

oncogenic kinases [30]. Parthenolide, a small molecule cancer inhibitor, inhibits cell growth, enhances apoptosis, and sensitizes cells to DPP treatment in gastric cancer cells [31]. Selumetinib, a drug used for treating type I neurofibromatosis in children, demonstrates effective therapeutic efficacy and tolerable safety in GC patients with MEK features or RAS gene alterations [32]. Tivantinib, an experimental small molecule anticancer drug, exhibits anticancer activity in GC cells by inhibiting c-MET or VEGFA amplification, thereby suppressing the VEGF signaling pathway and inducing apoptosis in gastric cancer cells [33]. Trametinib, a kinase inhibitor, restrains the development and metastasis of Gastric Neoplasia by targeting MAPK pathways [34]. Vorinostat, primarily utilized for treating cutaneous T-cell lymphoma, an histone deacetylase inhibitor, triggers death and autophagy in gastric cancer cell lines, presenting a potential therapeutic agent for gastric cancer [35].

IV. CONCLUSION

We have developed a transcriptome-based gastric adenocarcinoma computational drug repurposing pipeline. Initially, we selected four gene expression profiles related to cancer from the GEO database, comprising 258 RNA-seq datasets. By searching the corresponding DEG IDs on GEOexplorer, we obtained information on 1004 DEGs associated with these four gene expression profiles. Subsequently, we utilized the Uniprot database to identify the respective drug targets. For virtual screening, we downloaded over 10,000 structurally characterized drugs from DrugBank. Utilizing a deep neural network, we improved the prediction of drug-target interactions and constructed multiple omics networks. This approach facilitated the identification of core genes and targets for drug repurposing. We further explored the clinical trial evidence for these drugs in the field of cancer, assisting in drug ranking. Notably, Ursolic acid, Geldanamycin, Parthenolide, Selumetinib, Tivantinib, Trametinib, and Vorinostat emerged as the top-ranking drugs and were validated by published studies. This study demonstrates the potential of RepoGC in identifying novel drugs for gastric adenocarcinoma and provides an effective computational method for integrating transcriptomic data to facilitate rapid drug repurposing.

CONFLICT OF INTEREST

The author declares no conflict of interest.

REFERENCES

- [1] W. Gao, *et al.*, "A pipeline to call multilevel expression changes between cancer and normal tissues and its applications in repurposing drugs effective for gastric cancer," *BioMed Res. Int.*, 3451610, 2020.
- [2] E. C. Smyth, M. Nilsson, H. I. Grabsch, *et al.*, "Gastric cancer," *Lancet Lond. Engl.*, vol. 396, pp. 635–648, 2020.
- [3] C. R. Chong and D. J. Sullivan, "New uses for old drugs," *Nature*, vol. 448, pp. 645–646, 2007.
- [4] M. Rudrapal, *et al.*, "Drug Repurposing (DR): An emerging approach in drug discovery," *Drug Repurposing – Hypothesis, Molecular Aspects and Therapeutic Applications*, vol. 1, no. 1, 2020. doi:10.5772/intechopen.93193
- [5] Y. Cha, *et al.*, "Drug repurposing from the perspective of pharmaceutical companies," *Br. J. Pharmacol.*, vol. 175, pp. 168–180, 2018.
- [6] T. N. Jarada, J. G. Rokne, and R. Alhaji, "A review of computational drug repositioning: Strategies, approaches, opportunities, challenges, and directions," *J. Cheminformatics*, vol. 12, article number 46, 2020.
- [7] H. Luo, *et al.*, "DRAR-CPI: A server for identifying drug repositioning potential and adverse drug reactions via the chemical-protein interactome," *Nucleic Acids Res.*, vol. 39, pp. W492–W498, 2011.
- [8] K. Y.-L. Yap, A. Chan, W. K. Chui, and Y. Z. Chen, "Cancer informatics for the clinician: An interaction database for chemotherapy regimens and antiepileptic drugs," *Seizure*, vol. 19, pp. 59–67, 2010.
- [9] T. T. Ashburn and K. B. Thor, "Drug repositioning: Identifying and developing new uses for existing drugs," *Nat. Rev. Drug Discov.*, vol. 3, pp. 673–683, 2004.
- [10] J. Jia, *et al.*, "Mechanisms of drug combinations: Interaction and network perspectives," *Nat. Rev. Drug Discov.*, vol. 8, pp. 111–128, 2009.
- [11] T. Y. Demirtas, M. R. Rahman, M. C. Yurtsever, and E. Gov, "Forecasting gastric cancer diagnosis, prognosis, and drug repurposing with novel gene expression signatures," *Omics J. Integr. Biol.*, vol. 26, pp. 64–74, 2022.
- [12] H. M. Dönertaş, M. F. Valenzuela, L. Partridge, and J. M. Thornton, "Gene expression-based drug repurposing to target aging," *Aging Cell*, vol. 17, e12819, 2018.
- [13] R. Kumar and P. Saha, "A review on artificial intelligence and machine learning to improve cancer management and drug discovery," *Int. J. Res. Appl. Sci. Biotechnol.*, vol. 9, pp. 149–156, 2022.
- [14] C. Gloeckner, *et al.*, "Repositioning of an existing drug for the neglected tropical disease Onchocerciasis," *Proc. Natl. Acad. Sci. U. S. A.*, vol. 107, pp. 3424–3429, 2010.
- [15] S. Pushpakom, *et al.*, "Drug repurposing: Progress, challenges and recommendations," *Nat. Rev. Drug Discov.*, vol. 18, pp. 41–58, 2019.
- [16] J. T. Dudley, T. Deshpande, and A. J. Butte, "Exploiting drug-disease relationships for computational drug repositioning," *Brief Bioinform.*, vol. 12, pp. 303–311, 2011.
- [17] F. Iorio, T. Rittman, H. Ge, M. Menden, and J. Saez-Rodriguez, "Transcriptional data: A new gateway to drug repositioning?" *Drug Discov. Today*, vol. 18, pp. 350–357, 2013.
- [18] S. X. Ge, D. Jung, and R. Yao, "ShinyGO: A graphical gene-set enrichment tool for animals and plants," *Bioinforma. Oxf. Engl.*, vol. 36, pp. 2628–2629, 2020.
- [19] A. Liberzon, *et al.*, "The molecular signatures database hallmark gene set collection," *Cell Syst.*, vol. 1, pp. 417–425, 2015.
- [20] H. Araki, C. Knapp, P. Tsai, and C. Print, "GeneSetDB: A comprehensive meta-database, statistical and visualisation framework for gene set analysis," *FEBS Open Bio.*, vol. 2, pp. 76–82, 2012.
- [21] A. Fabregat, *et al.*, "The reactome pathway knowledgebase," *Nucleic Acids Res.*, vol. 44, pp. D481–D487, 2016.
- [22] M. Kanehisa, M. Furumichi, M. Tanabe, *et al.*, "KEGG: New perspectives on genomes, pathways, diseases and drugs," *Nucleic Acids Res.*, vol. 45, pp. D353–D361, 2017.
- [23] P. Willett, J. M. Barnard, and G. M. Downs, "Chemical similarity searching," *J. Chem. Inf. Comput. Sci.*, vol. 38, pp. 983–996, 1998.
- [24] D. Rogers and M. Hahn, "Extended-connectivity fingerprints," *J. Chem. Inf. Model.*, vol. 50, pp. 742–754, 2010.
- [25] M. Heinzinger, *et al.*, "Modeling aspects of the language of life through transfer-learning protein sequences," *BMC Bioinformatics*, vol. 20, article number 723, 2019.
- [26] K. Huang, *et al.*, "DeepPurpose: A deep learning library for drug-target interaction prediction," *Bioinformatics*, vol. 36, pp. 5545–5547, 2020.
- [27] C. Sansom, "Role of stomach acid in gastric cancer," *Lancet Oncol.*, vol. 6, 2005.
- [28] B. Messina, *et al.*, "Hippo pathway dysregulation in gastric cancer: From Helicobacter pylori infection to tumor promotion and progression," *Cell Death Dis.*, vol. 14, pp. 1–12, 2023.
- [29] X. Wang, *et al.*, "Ursolic acid inhibits proliferation and induces apoptosis of cancer cells in vitro and in vivo," *J. Biomed. Biotechnol.*, 419343, 2011.

- [30] H. Chen, L.-Q. Li, and D. Pan, "Geldanamycin induces apoptosis in human gastric carcinomas by affecting multiple oncogenic kinases that have synergic effects with TNF-related apoptosis-inducing ligand," *Oncol. Lett.*, vol. 10, pp. 3732–3736, 2015.
- [31] M. Liu, Y. Yang, D. Liu, Y. Cao, and Y. Li, "Parthenolide increases the sensitivity of gastric cancer cells to chemotherapy," *J. Tradit. Chin. Med. Chung Tsa Chih Ying Wen Pan*, vol. 40, pp. 908–916, 2020.
- [32] J. Lee, *et al.*, "Selumetinib plus docetaxel as second-line chemotherapy in KRAS mutant, KRAS amplified or MEK signatred gastric cancer patients: First arm of the umbrella trial in GC though the molecular screening, VIKTORY trial," *J. Clin. Oncol.*, vol. 36, pp. 4061–4061, 2018.
- [33] B. J. Kim, *et al.*, "Tivantinib inhibits the VEGF signaling pathway and induces apoptosis in gastric cancer cells with c-MET or VEGFA amplification," *Invest. New Drugs*, vol. 38, pp. 1633–1640, 2020.
- [34] J. Yamasaki, *et al.*, "MEK inhibition suppresses metastatic progression of KRAS-mutated gastric cancer," *Cancer Sci.*, vol. 113, pp. 916–925, 2022.
- [35] S. Claerhout, *et al.*, "Gene expression signature analysis identifies vorinostat as a candidate therapy for gastric cancer," *PloS One*, vol. 6, e24662, 2011.
- [36] C.-H. Lee, *et al.*, "Isoliquiritigenin inhibits gastric cancer stemness, modulates tumor microenvironment, and suppresses tumor growth through glucose-regulated protein 78 downregulation," *Biomedicines*, vol. 10, 1350, 2022.
- [37] R. C. Montenegro, *et al.*, "Identification of molecular targets for the targeted treatment of gastric cancer using dasatinib," *Oncotarget*, vol. 11, pp. 535–549, 2020.
- [38] L. Du, Z. Che, and A. Wang-Gillam, "Promising therapeutics of gastrointestinal cancers in clinical trials," *J. Gastrointest. Oncol.*, vol. 8, pp. 524–533, 2017.
- [39] Z. Wang, *et al.*, "Tegaserod maleate suppresses the growth of gastric cancer in vivo and in vitro by targeting MEK1/2," *Cancers*, vol. 14, 3592, 2022.
- [40] S. Keller, *et al.*, "Effects of trastuzumab and afatinib on kinase activity in gastric cancer cell lines," *Mol. Oncol.*, vol. 12, pp. 441–462, 2018.
- [41] T. Aparicio, *et al.*, "The activity of crizotinib in chemo-refractory met-amplified esophageal and gastric adenocarcinomas: Results from the AcSé-Crizotinib program," *Target. Oncol.*, vol. 16, pp. 381–388, 2021.

Copyright © 2024 by the authors. This is an open access article distributed under the Creative Commons Attribution License ([CC BY-NC-ND 4.0](https://creativecommons.org/licenses/by-nc-nd/4.0/)), which permits use, distribution and reproduction in any medium, provided that the article is properly cited, the use is non-commercial and no modifications or adaptations are made.